32ND INTERNATIONAL COSMIC RAY CONFERENCE, BEIJING 2011

Modeling of the galactic cosmic-ray anisotropy at TeV energies

M. AMENOMORI[1], X. J. BI[2], D. CHEN[3], W. Y. CHEN[2], S. W. CUI[4], DANZENGLUOBU[5], L. K. DING[2], X. H. DING[5], C. F. FENG[6], ZHAOYANG FENG[2], Z. Y. FENG[7], Q. B. GOU[2], H. W. GUO[5], Y. Q. GUO[2], H. H. HE[2], Z. T. HE[4,2], K. HIBINO[8], N. HOTTA[9], HAIBING HU[5], H. B. HU[2], J. HUANG[2], W. J. LI[2,7], H. Y. JIA[7], L. JIANG[2], F. KAJINO[10], K. KASAHARA[11], Y. KATAYOSE[12], C. KATO[13], K. KAWATA[3], LABACIREN[5], G. M. LE[2], A. F. LI[14,6,2], C. LIU[2], J. S. LIU[2], H. LU[2], X. R. MENG[5], K. MIZUTANI[11,15], K. MUNAKATA[13], H. NANJO[1], M. NISHIZAWA[16], M. OHNISHI[3], I. OHTA[17], S. OZAWA[11], X. L. QIAN[6,2], X. B. QU[2], T. SAITO[18], T. Y. SAITO[19], M. SAKATA[10], T. K. SAKO[12], J. SHAO[2,6], M. SHIBATA[12], A. SHIOMI[20], T. SHIRAI[8], H. SUGIMOTO[21], M. TAKITA[3], Y. H. TAN[2], N. TATEYAMA[8], S. TORII[11], H. TSUCHIYA[22], S. UDO[8], H. WANG[2], H. R. WU[2], L. XUE[6], Y. YAMAMOTO[10], Z. YANG[2], S. YASUE[23], A. F. YUAN[5], T. YUDA[3], L. M. ZHAI[2], H. M. ZHANG[2], J. L. ZHANG[2], X. Y. ZHANG[6], Y. ZHANG[2], YI ZHANG[2], YING ZHANG[2], ZHAXISANGZHU[5], X. X. ZHOU[7] (THE TIBET ASγ COLLABORATION)

[1]*Department of Physics, Hirosaki University, Hirosaki 036-8561, Japan*
[2]*Key Laboratory of Particle Astrophysics, Institute of High Energy Physics, Chinese Academy of Sciences, Beijing 100049, China*
[3]*Institute for Cosmic Ray Research, University of Tokyo, Kashiwa 277-8582, Japan*
[4]*Department of Physics, Hebei Normal University, Shijiazhuang 050016, China*
[5]*Department of Mathematics and Physics, Tibet University, Lhasa 850000, China*
[6]*Department of Physics, Shandong University, Jinan 250100, China*
[7]*Institute of Modern Physics, SouthWest Jiaotong University, Chengdu 610031, China*
[8]*Faculty of Engineering, Kanagawa University, Yokohama 221-8686, Japan*
[9]*Faculty of Education, Utsunomiya University, Utsunomiya 321-8505, Japan*
[10]*Department of Physics, Konan University, Kobe 658-8501, Japan*
[11]*Research Institute for Science and Engineering, Waseda University, Tokyo 169-8555, Japan*
[12]*Faculty of Engineering, Yokohama National University, Yokohama 240-8501, Japan*
[13]*Department of Physics, Shinshu University, Matsumoto 390-8621, Japan*
[14]*School of Information Science and Engineering, Shandong Agriculture University, Taian 271018, China*
[15]*Saitama University, Saitama 338-8570, Japan*
[16]*National Institute of Informatics, Tokyo 101-8430, Japan*
[17]*Sakushin Gakuin University, Utsunomiya 321-3295, Japan*
[18]*Tokyo Metropolitan College of Industrial Technology, Tokyo 116-8523, Japan*
[19]*Max-Planck-Institut für Physik, München D-80805, Deutschland*
[20]*College of Industrial Technology, Nihon University, Narashino 275-8576, Japan*
[21]*Shonan Institute of Technology, Fujisawa 251-8511, Japan*
[22]*RIKEN, Wako 351-0198, Japan*
[23]*School of General Education, Shinshu University, Matsumoto 390-8621, Japan*
tsako@icrr.u-tokyo.ac.jp

Abstract: A possible origin of the large-scale anisotropy of TeV galactic cosmic rays is discussed. It can be well modeled by a superposition of the Global Anisotropy and the Midscale Anisotropy. The Global Anisotropy would be generated by galactic cosmic rays interacting with the magnetic field in the local interstellar space of a few parsec scale surrounding the heliosphere. On the other hand, the Midscale Anisotropy would be caused by the modulation of galactic cosmic rays in the heliotail. The Midscale Anisotropy can be expressed as two intensity enhancements placed along the Hydrogen Deflection Plane, each symmetrically centered away from the heliotail direction. It is found that the separation angle between the heliotail direction and each of the two intensity enhancements monotonously decreases as energy increases from 4 TeV to 30 TeV.

Keywords: Tibet, galactic cosmic rays, anisotropy, TeV energies

1 Introduction

Past cosmic-ray experiments that observed cosmic-ray anisotropy in the sidereal time frame consistently reported that in the anisotropy there are two distinct broad structures with an amplitude of $\sim$0.1%; one is a deficit in the cosmic-ray flux called "loss-cone", distributed around 150° to 240° in Right Ascension, and the other an excess called "tail-in", distributed around 40° to 90° in Right Ascension. Recent underground muon and air-shower experiments are studying the anisotropy in a great detail at multi-TeV energies [1, 2, 3]. It is considered that the anisotropy of galactic cosmic rays at TeV energies reflects the structure of the local interstellar magnetic field surrounding the heliosphere, since the trajectories of charged cosmic rays are deflected and scrambled by the local interstellar magnetic field while they are traveling through the interstellar medium.

2 Analysis and Results

The Tibet air-shower array has been operating successfully since 1990 at 90.522° E, 30.102° N and 4300 m above sea level. The air-shower events collected during the period from November 1999 through December 2008 (1916 live days) are used for analysis. After our standard data selections, 4.5×10^{10} events are left with a modal energy of 7 TeV. More details of the Tibet air-shower experiment and our analysis method are described in our separate papers [1, 4, 5]. The main systematic error to be accounted for is the amplitude of the anisotropy observed in the anti-sidereal time frame (364.2422 cycles/yr), because a possible seasonal change of the solar daily variation due to solar activities might produce a spurious variation in the sidereal time frame, which can be estimated by the daily variation observed in the anti-sidereal time frame. The root mean square of the anti-sidereal anisotropy in each declination band is calculated and added to the statistical error for the sidereal anisotropy in the corresponding declination band. Shown in Fig.1(a) is the relative intensity map obtained in $5^\circ\times5^\circ$ pixels, which we model in terms of two components as [5]:

$$I_{n,m} = I^{GA}_{n,m} + I^{MA}_{n,m}, \tag{1}$$

where $I^{GA}_{n,m}$ and $I^{MA}_{n,m}$ respectively denote the intensities of the Global Anisotropy (GA) and the Midscale Anisotropy (MA) of the (n, m) pixel in the equatorial coordinate system. The GA component $I^{GA}_{n,m}$ is written as the combination of a uni-directional flow (UDF) and a bi-directional flow (BDF):

$$\begin{aligned} I^{GA}_{n,m} &= a_{1\perp}\cos\chi_1(n,m:\alpha_1,\delta_1) \\ &\quad + a_{1\parallel}\cos\chi_2(n,m:\alpha_2,\delta_2) \\ &\quad + a_{2\parallel}\cos^2\chi_2(n,m:\alpha_2,\delta_2). \end{aligned} \tag{2}$$

In Eq.(2), the orientation (α_2, δ_2) denotes the reference axis of the BDF, and $a_{2\parallel}$ the amplitude of the BDF. The UDF is decomposed into two: one that is parallel to the BDF and has an amplitude of $a_{1\parallel}$, and the other that is perpendicular to the BDF, parallel to the axis (α_1, δ_1), and has an amplitude of $a_{1\perp}$. The χ_1 denotes the angular distance of the center of the (n,m) pixel measured from the reference axis (α_1, δ_1), and the χ_2 denotes that measured from the axis (α_2, δ_2). Fig.1(b) shows the anisotropy map reproduced by attempting to fit Fig.1(a) with $I^{GA}_{n,m}$ alone. Although Fig.1(b) successfully reproduces the global "tail-in" and "loss-cone" structures, there remains the midscale anisotropy as can be seen in Fig.1(c). The $I^{MA}_{n,m}$, incorporated to model the residual midscale anisotropy, is expressed as:

$$\begin{aligned} I^{MA}_{n,m} = \Bigg\{ & b_1\exp\left(-\frac{(\phi_{n,m}-\Phi)^2}{2\sigma^2_\phi}\right) + \\ & b_2\exp\left(-\frac{(\phi_{n,m}+\Phi)^2}{2\sigma^2_\phi}\right)\Bigg\}\exp\left(-\frac{\theta^2_{n,m}}{2\sigma^2_\theta}\right), \end{aligned} \tag{3}$$

where b_1 and b_2 denote the amplitudes of the two excesses along the best-fit plane with the heliotail direction on it, both of which are symmetrically centered away from the heliotail direction by an angle Φ along the plane. The σ_ϕ and σ_θ denote the widths of the excesses parallel and perpendicular to the best-fit plane, respectively. The $\phi_{n,m}$ and $\theta_{n,m}$ denote the "longitude" of the center of the (n,m) pixel measured from the heliotail direction and its "latitude" measured from the best-fit plane, respectively. Fig.1(e) and (f) show the reproduced anisotropy and the residual anisotropy when we fit Fig.1(a) with $I^{GA}_{n,m}+I^{MA}_{n,m}$. The $I^{MA}_{n,m}$ extracted from Fig.1(e) is shown in Fig.1(d). Note that the obtained best-fit plane along which the MA is assumed is fairly consistent with the Hydrogen Deflection Plane (HDP) suggested by Gurnett et al. [6], which contains the directions of the interstellar wind velocity and the interstellar magnetic field upstream the helionose; the angle difference between the direction normal to our best-fit plane and that to Gurnett's HDP is only 2.1°. The best-fit parameters in Eq.(2) and Eq.(3) are listed in Table 1.

3 Discussions

The GA can be interpreted as follows (for details, see [5, 7]). The local interstellar space of scale $\sim$2 pc surrounding the heliosphere would be responsible for the GA. The BDF is produced by cosmic rays drifting parallel to the Local Interstellar Magnetic Field (LISMF) line into the heliosphere from outside the Local Interstellar Cloud surrounding the heliosphere. The UDF, perpendicular to the LISMF ($a_{1\perp} \gg a_{1\parallel}$) with an amplitude comparable to that of the BDF ($a_{1\perp} \simeq a_{2\parallel}$), can be produced by a diamagnetic drift arising from a spatial density gradient ($\nabla n/n$) of galactic cosmic rays in the LISMF.

A sketch of a possible mechanism for the MA is shown in Fig.2(a). During the period of the data we analyzed, the orientation of the magnetic field in the heliotail $B_{\rm helio}$ is directed toward (away from) the Sun in the northern (southern) hemisphere. Suppose, for simplicity, that the $B_{\rm helio}$

surrounding the solar system is uniform within the spatial scale L toward the heliotail direction. Then the uniform $B_{\rm helio}$ bends the trajectories of cosmic rays propagating along the HDP from the heliotail direction, leading them to the solar system. A simple geometrical consideration gives the following relation:

$$\begin{aligned} L\,[\mathrm{AU}] &= R_L\,[\mathrm{AU}]\,\sin\Phi \\ &= 206(E\,[\mathrm{TeV}]/B_{\rm helio}\,[\mu\mathrm{G}])\sin\Phi, \quad (4) \end{aligned}$$

where R_L is the Larmor radius of cosmic rays with energy E in $B_{\rm helio}$. This equation implies that $\sin\Phi \propto 1/E$ if L is independent of energy. The observed energy dependence of $\sin\Phi$, shown in Fig.2(b), gives the following function:

$$\sin\Phi = (0.68 \pm 0.04)\,(E/10\,[\mathrm{TeV}])^{-0.20\pm0.08}, \quad (5)$$

suggesting $L \propto E^{0.8}$. This energy dependence of L might result from actual complex spatial structures of $B_{\rm helio}$. These structures could be identified in the future by studies on the cosmic-ray transport in $B_{\rm helio}$ by means of Magneto-Hydrodynamic simulations [11]. Substituting Eq.(5) into Eq.(4) and assuming $B_{\rm helio} = 10\mu$G, the following equation holds:

$$L\,[\mathrm{AU}] = (140 \pm 8)\,(E/10\,[\mathrm{TeV}])^{0.80\pm0.08}, \quad (6)$$

Eq.(6) implies that in the energy range of 4$-$30 TeV $B_{\rm helio}$ within $\sim$70 AU to $\sim$340 AU from the Sun is responsible for the MA. The MA being placed along the HDP suggests that it possibly originates from the modulation of galactic cosmic rays in $B_{\rm helio}$. Another candidate for the heliospheric signature could be the excess region first reported as the "hot-spot" by the Milagro experiment [12]. This region corresponds to the pixel in Fig.1(a) centered at (72.5°, 17.5°), close to the heliotail, observed with the highest significance 9.06σ among all the pixels. The excess region is so collimated that it is difficult to construe it as a cosmic-ray inflow along the neutral sheet that separates $B_{\rm helio}$ between the northern and southern hemispheres. The Milagro experiment reported that the "hot-spot" has a localized spatial extension with a half-width of $2.6^\circ \pm 0.3^\circ$ and a half-length of $7.6^\circ \pm 1.1^\circ$. It should be noted here that the size of such a small-scale structure is greatly susceptible to the size and shape of the analysis window for background estimation to subtract the large-scale anisotropy superposed on the structure.

4 Conclusions

We discussed the origin of the large-scale anisotropy of galactic cosmic rays at TeV energies. It can be well modeled by a superposition of the Global Anisotropy and the Midscale Anisotropy. The GA, for which the local interstellar space of a few parsec scale surrounding the heliosphere would be responsible, is expressed as the combination of a UDF and a BDF of galactic cosmic rays. The BDF is produced by the drift of cosmic rays parallel to the LISMF line into the heliosphere from outside the Local Interstellar Cloud surrounding the heliosphere. Meanwhile, the UDF, which is perpendicular to the LISMF, can be produced by a diamagnetic drift arising from a spatial density gradient of galactic cosmic rays in the LISMF.

The MA, for which in the energy range of 4$-$30 TeV $B_{\rm helio}$ within $\sim$70 AU to $\sim$340 AU from the Sun is responsible, is expressed as two cosmic-ray intensity enhancements placed along the HDP and symmetrically centered away from the heliotail direction, with the separation angle between the heliotail direction and each of the two enhancements decreasing monotonously as energy increases. The MA being placed along the HDP, which contains the directions of the interstellar wind velocity and the interstellar magnetic field surrounding the heliosphere, suggests that it possibly originates from the modulation of galactic cosmic rays in the magnetic field of the heliotail.

5 Acknowledgments

The collaborative experiment of the Tibet Air Shower Arrays has been performed under the auspices of the Ministry of Science and Technology of China and the Ministry of Foreign Affairs of Japan. This work was supported in part by a Grant-in-Aid for Scientific Research on Priority Areas from the Ministry of Education, Culture, Sports, Science and Technology, by Grants-in-Aid for Science Research from the Japan Society for the Promotion of Science in Japan, and by the Grants from the National Natural Science Foundation of China and the Chinese Academy of Sciences.

References

[1] M. Amenomori *et al.*, Science, 2006, 314: 439-443
[2] G. Guillian *et al.*, Phys. Rev. D, 2007, 75(6): 0620031-06200317
[3] R. Abbasi *et al.*, arXiv:1105.2326v1
[4] M. Amenomori *et al.*, AIP Conf. Proc., 2007, 932: 283-289
[5] K. Munakata *et al.*, arXiv:0909.1026
[6] D. Gurnett *et al.*, AIP Conf. Proc., 2006, 858: 129-134
[7] Y. Mizoguchi *et al.*, arXiv:0909.1029
[8] R. Lallement *et al.*, Science, 2005, 307(5714): 1447-1449
[9] P. Frisch, Space Sci. Rev., 1996, 78: 213-222
[10] J. Heerikhuisen *et al.*, ApJL, 2010, 708(2): L126-L130
[11] H. Washimi *et al.*, ApJL, 2007, 670(2): L139-L142
[12] A. Abdo *et al.*, PRL, 2008, 101(22): 2211011-2211015

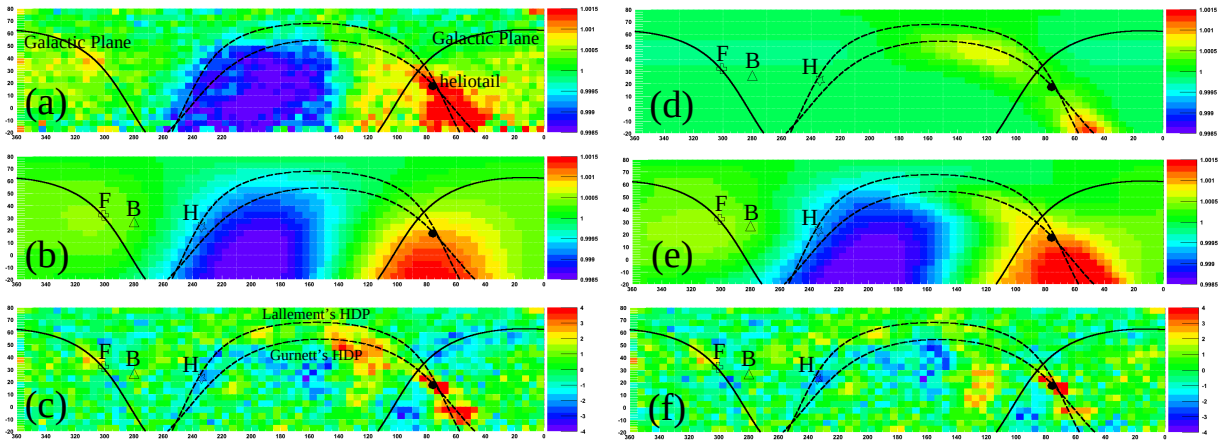

Figure 1: Two-dimensional anisotropy maps of galactic cosmic rays observed and reproduced at the modal energy of 7 TeV. Each panel shows the relative intensity map or the significance map in $5^\circ \times 5^\circ$ pixels in the equatorial coordinate system.
(a): the observed cosmic-ray intensity ($I^{obs}_{n,m}$), (b): the best-fit Global Anisotropy (GA) component ($I^{GA}_{n,m}$), (c): the significance map of the residual anisotropy after subtracting $I^{GA}_{n,m}$ from $I^{obs}_{n,m}$, (d): the best-fit Midscale Anisotropy (MA) component ($I^{MA}_{n,m}$), (e): the best-fit GA+MA components ($I^{GA}_{n,m} + I^{MA}_{n,m}$), and (f): the significance map of the residual anisotropy after subtracting $I^{GA}_{n,m} + I^{MA}_{n,m}$ from $I^{obs}_{n,m}$.
The solid black curves represent the galactic plane. The dashed black curves represent the Hydrogen Deflection Plane reported by Gurnett *et al.* [6] and Lallement *et al.* [8]. The heliotail direction (α, δ) = (75.9°, 17.4°) is indicated by the black filled circle. The open cross and the inverted star with the attached characters "F" and "H" represent the orientation of the local interstellar magnetic field (LISMF) by Frisch [9] and by Heerikhuisen *et al.* [10], respectively. The open triangle with "B" indicates the orientation of the best-fit bi-directional cosmic-ray flow (BDF) obtained in this paper.

Table 1: Best-fit parameters in Eq.(2) and Eq.(3) for the 2D galactic-cosmic-ray anisotropy map observed at 7 TeV.

Global Anisotropy (GA)						
$a_{1\perp}$ (%)	$a_{1\parallel}$ (%)	$a_{2\parallel}$ (%)	$\alpha_1(^\circ)$	$\delta_1(^\circ)$	$\alpha_2(^\circ)$	$\delta_2(^\circ)$
0.139 ± 0.002	0.007 ± 0.002	0.131 ± 0.004	33.3 ± 1.1	38.4 ± 1.2	279.9 ± 0.9	-26.7 ± 2.0
Midscale Anisotropy (MA)						
b_1 (%)	b_2 (%)	$\sigma_\phi(^\circ)$	$\sigma_\theta(^\circ)$	Φ (°)		
0.154 ± 0.018	0.092 ± 0.006	24.5 ± 1.1	10.7 ± 0.8	49.2 ± 1.4		

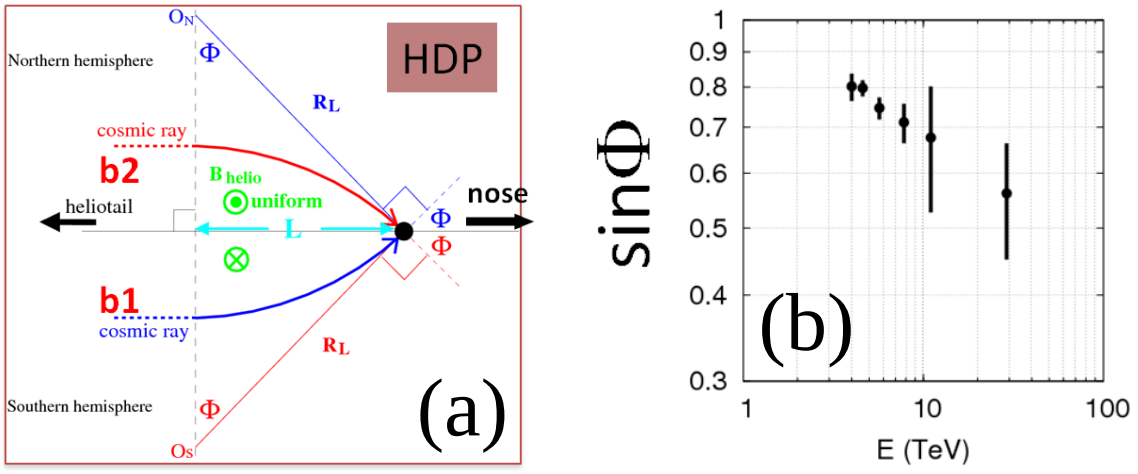

Figure 2: (a): a possible mechanism for the Midscale Anisotropy. (b): the observed energy dependence of sinΦ.